Distinct genetic origins of eumelanin intensity and barring patterns in cichlid fishes

A. Allyson Brandon[1], Cassia Michael[1], Aldo Carmona Baez[2], Emily C. Moore[2,3], Patrick J. Ciccotto[4], Natalie B. Roberts[2], Reade B. Roberts[2], and Kara E. Powder[1]*

[1] Department of Biological Sciences, Clemson University, Clemson, SC 29634, USA.
[2] Department of Biological Sciences, and Genetics and Genomics Academy, North Carolina State University, Raleigh, NC 27695, USA.
[3] Department of Biological Sciences, University of Montana, Missoula, MT 59812, USA.
[4] Department of Biology, Warren Wilson College, Swannanoa, NC 28778, USA.

Corresponding Author:
Department of Biological Sciences
Clemson University
055A Life Science Facility
190 Collings Street
Clemson, SC 29634
Tel: 864-656-3196
Email: kpowder@clemson.edu

RUNNING TITLE

Barring variation in cichlids

KEYWORDS: quantitative trait loci, pigmentation, Cichlidae, adaptation, melanophore, coloration

ABSTRACT

Pigment patterns are incredibly diverse across vertebrates and are shaped by multiple selective pressures from predator avoidance to mate choice. A common pattern across fishes, but for which we know little about the underlying mechanisms, is repeated melanic vertical bars. In order to understand genetic factors that modify the level or pattern of vertical barring, we generated a genetic cross of 322 F_2 hybrids between two cichlid species with distinct barring patterns, *Aulonocara koningsi* and *Metriaclima mbenjii*. We identify 48 significant quantitative trait loci that underlie a series of seven phenotypes related to the relative pigmentation intensity, and four traits related to patterning of the vertical bars. We find that genomic regions that generate variation in the level of eumelanin produced are largely independent of those that control the spacing of vertical bars. Candidate genes within these intervals include novel genes and those newly-associated with vertical bars, which could affect melanophore survival, fate decisions, pigment biosynthesis, and pigment distribution. Together, this work provides insights into the regulation of pigment diversity, with direct implications for an animal's fitness and the speciation process.

INTRODUCTION

Coloration of animals has long fascinated both scientists and non-scientists alike. For centuries, scientists have asked questions about the underlying genetic control, diversity of variation, and ecological relevance of changes in pigmentation (Castle & Allen, 1903; Darwin, 1871; Wright, 1917). The rich collection of hues, spots, stripes, and bars of animals integrate both natural and sexual selective pressures (Brandon,

Almeida, & Powder, 2023; Hoekstra, 2006; Hubbard, Uy, Hauber, Hoekstra, & Safran, 2010; Maan & Sefc, 2013). Pigmentation patterns are related to crypsis and predator avoidance, mate choice, color-mediated aggression, social dominance and competitive interactions, and collective animal behaviors such as schooling or shoaling in fishes (Brandon et al., 2023; Cuthill et al., 2017; Eizirik & Trindade, 2021; Hubbard et al., 2010; Korzan & Fernald, 2007; Maan & Sefc, 2013; Parichy, 2021; Protas & Patel, 2008; Sefc, Brown, & Clotfelter, 2014). Through this, these traits directly affect reproductive success, fitness, and speciation (Wagner, Harmon, & Seehausen, 2012), and the ultimate result is an incredible array of color pattern variation across animals.

One clade with notable variation in pigmentation is cichlid fishes, which have undergone a rapid and extensive adaptive radiation (Powder & Albertson, 2016; Santos, Lopes, & Kratochwil, 2023). Cichlids exhibit dramatic variation in their coloration, with variation due to species, sex, and geography (Konings, 2016; Maan & Sefc, 2013). The evolution of pigmentation is particularly important in cichlids, where sexual selection on divergent nuptial coloration appears to maintain pre-mating reproductive isolation among the most recently evolved species (Danley & Kocher, 2001). Much work has been done to begin to understand the molecular origins of the rich palette found across cichlids. Various genomic approaches have identified genetic loci that regulate black blotches (Roberts, Moore, & Kocher, 2017; Roberts, Ser, & Kocher, 2009), dark horizontal stripes (Kratochwil et al., 2018), yellow egg spots (Salzburger, Braasch, & Meyer, 2007; Santos et al., 2014), black and yellow coloration of the fins (Ahi & Sefc, 2017; O'Quin, Drilea, Conte, & Kocher, 2013), golden morphs (Wang, Xu, Kocher, Li, & Wang, 2022),

albinism (Kratochwil, Urban, & Meyer, 2019), and even modularity in patterns across the flank (Albertson et al., 2014). However, one pigment phenotype that is understudied is the most common pigment pattern, dark vertical barring (Santos et al., 2023). In contrast to horizontal stripes, whose presence and absence is controlled by a master switch gene *agouti-related peptide 2* (*agrp2,* also known as *asip2b*) (Kratochwil et al., 2018), the presence of barring in cichlids is predicted to be polygenic (Gerwin, Urban, Meyer, & Kratochwil, 2021). These darkly pigmented bars are primarily due to a population of melanin producing cells called melanophores. Melanophores originate from trunk neural crest cells, as do other pigment cells in teleosts including xanthophores that generate red/yellow pigment and iridophores which are reflective (Parichy, 2021).

Here, we sought to determine the underlying genetic regulators of variation in vertical bar pigmentation. To accomplish this, we generated a genetic mapping cross of two Lake Malawi cichlids with alternate barring phenotypes. *Aulonocara koningsi* has high-contrast bars across its body, and *Metriaclima mbenjii* has fewer and fainter bars, with little contrast between bars and the background pigment levels (Figure 1a-b). By crossing two species that both display vertical barring, we set out to identify factors that alter the intensity and spacing of these bars, rather than master regulators governing their presence. In particular, we expected that one set of genomic regions would regulate where melanophores were located and the pattern of the bars, and a separate set of genes would independently regulate the levels of black/brown eumelanin being produced and dispersed from melanophores. We identify genetic intervals with

candidate genes that are redeployed across vertebrates to regulate barring as well as other pigment phenotypes, as well as a series of additional genetic regions that are novel regulators of barring. Together, these data provide insights into the genetic and molecular underpinnings of pigment biodiversity, which lies at the intersection of a series of selective pressures that shape an animal's ecology and evolution.

MATERIALS AND METHODS

Experimental cross

All animal care was conducted under approved IACUC protocol 14-101-O at North Carolina State University. A hybrid cross was generated from a single female *Metriaclima mbenjii* that was crossed to two male *Aulonocara koningsi*. The inadvertent inclusion of two grandsires resulted from an unexpected fertilization, as these animals externally fertilize. We discuss how this was accounted for during genotyping in the section *Genotyping and linkage map generation*. A single F_1 family from this cross was subsequently in-crossed to generate an F_2 hybrid mapping population. F_2 hybrids were raised in density-controlled aquaria and with standardized measured feedings until around sexual maturity (five months of age), at which time they were sacrificed for analysis. The sex of each animal was determined based on a combination of gonad dissections at sacrifice and genotype at an XY locus on LG7 that solely determined sex in this cross (Peterson, Cline, Moore, Roberts, & Roberts, 2017; Ser, Roberts, & Kocher, 2010). Sex was omitted for animals with ambiguity or discrepancies between these calls (8.77% of animals), resulting in a set of 479 hybrids with 48.74% females.

Imaging and filtering of data set

Images were taken of animals that were freshly sacrificed via cold buffered 100 mg/L MS-222. Euthanasia in cold solution relaxed chromatophores in the skin to maximize black/brown eumelanin-based pigmentation (Albertson et al., 2014). Whole fish photographs were taken using a uniform setup, with standard lighting conditions in a lightbox with a mirrorless digital camera (Olympus). All images included a scale bar and a gray scale color standard. Images were color balanced in Adobe Photoshop (version 22.0.0 or after) using the black and white segments of the color standard. From the total data set of 10 parentals of *Aulonocara koningsi*, 10 parentals of *Metriaclima mbenjii*, and 479 F_2 hybrids, we omitted fish that exhibited two pigmentation phenotypes. First, *Metriaclima mbenjii* has a high percentage of animals that carry the 'orange blotch' (OB) phenotype, which results in marbled melanophore blotches rather than distinct barring (Konings, 2016; Roberts et al., 2017; Roberts et al., 2009). To enable analysis of barring patterns, we therefore removed 4 OB *Metriaclima mbenjii* parentals and 96 OB F_2 hybrids. We further removed 65 hybrids that were heavily melanic to the degree that the eye was not distinguishable from the head or flank and thus anatomical landmarks used for additional processing were not visible. The final data set after this filtering included 10 *Aulonocara koningsi* parentals, 6 *Metriaclima mbenjii* parentals, and 322 F_2 hybrids (48.97% female).

Isolation and quantification of pigmented region

Images were rotated so a horizontal guideline aligned the midline of the caudal peduncle and the tip of the snout. A second horizontal guideline was added at the top of the caudal

peduncle. From this image, a region was extracted for the remainder of the analysis (indicated by orange outlines in Figure 1a-b). This region was 10 pixels high with the ventral side aligned with the guide at the top of the caudal peduncle, the opercle at the anterior end, and the dorsal fin on the posterior end (Figure 1a-b). This standardized region of the body was chosen as it has a barring pattern representative of the entire flank and avoids areas that included the pectoral fin in a portion of images, which introduced variation in measurements of pigmentation.

The image of the isolated region was uploaded to FIJI software (version 2.9.0) (Schindelin et al., 2012), where it was converted to 32-bit grayscale. Following (Greenwood et al., 2011; O'Quin, Drilea, Roberts, & Kocher, 2012), the Plot Profile command in FIJI was used to convert the image to a numerical gray value from 0 (pure black) to 255 (pure white), averaging the values of the 10 pixels in each column (Figure 1). Isolated regions had an average width of 174 $\pm$ 36 pixels, which equated to 1.26 $\pm$ 0.26 centimeters or 30.6 $\pm$ 3.8 % of the total length (snout to caudal peduncle) of the animal.

Quantification of melanic traits

Outputted data from Plot Profile in FIJI were analyzed in either R or with a custom perl script available at https://github.com/kpowder/Biology2022. The perl script used two criteria to define bars and interbars (defined as the region between bars) (Figure 1a-b) based on empirical testing of four *Aulonocara koningsi* parentals, four *Metriaclima mbenji* parentals, and four F_2 hybrids, all randomly-chosen. Both cutoffs described below were selected as they accurately represented the barring pattern that was observed by eye on

this test data set (Figure S1). First, we used the average intensity value to define bar regions, with gray intensity value less than (i.e., darker than) the average considered within a bar, and gray intensity value greater than this average considered within an interbar (Figure 1a-b and Figure S1). Second, to minimize overcounting of bars due to variation in pigment intensity from one pixel to the next, we required a bar to have at least 5 sequential pixels with intensity values below the average, and define the end of the bar as 5 pixels in a row above the average gray intensity value.

From the Plot Profile data and output of the perl script, we calculated seven measures related to variation in the levels of eumelanin produced: darkest intensity, lightest intensity, range of intensity, covariance of intensity measure with anterior-posterior position, the average intensity of bars, the average intensity of interbars, and the differential intensity between bars and interbars (Figure 1c). We note that an increased range of intensity, covariance, and differential intensity between bars and interbars are characteristic of animals with more discrepancy between bars and interbars (that is, highly melanic bars on very pale backgrounds). We also calculated four measures based around variation in the pattern of what regions of the body had bars: the total number of bars, the average width of bars, the average width of interbars, and the percent of barring, measured as the total length of regions classified as bars divided by the total length of the isolated region (Figure 1d).

Statistical analysis of pigment measures

For each individual, the standard length of the animal was measured in FIJI as the number of pixels between the snout and the caudal peduncle, which was converted into absolute length in centimeters using a scale bar included in each picture. To remove the effects of allometry on pigment phenotypic measures, all measurements were converted into residual data by normalizing to the standard length, using a dataset including both parentals and hybrids. Analyses including linear normalization, ANOVAs, Tukey's Honest Significant Difference post-hoc tests, and Pearson's correlations were conducted in R (version 3.5.2 or higher).

Genotyping and linkage map generation

Isolation, sequencing, and genotype calls are fully described in (DeLorenzo et al., 2023). Briefly, genomic DNA was extracted from caudal fin tissue, used to generate ddRADseq libraries, and sequenced on an Illumina HiSeq with 100bp paired end reads. Following demultiplexing and filtering of low-quality reads, reads were aligned to the *Metriaclima zebra* UMD2a reference genome and genotypes were called for those markers that had alternative alleles between the parents (i.e., AA x BB) and had a stack depth of 3. As mentioned above, an inadvertent fertilization event led to two grandsires in this cross. To focus on species-level genetic contributions, markers were excluded if *Aulonocara* sires had discrepant genotypes or Hardy-Weinberg equilibrium was not met. Any phenotypic effects of genetic variation from a single grandsire (that is, intraspecies variation) is expected to be diluted in this cross and therefore not be identified in the subsequent QTL mapping described in the following section.

Generation of the linkage map is fully described in (DeLorenzo et al., 2023), was built in R (version 4.0.3) with the package R/qtl (version 1.44-9) (Broman, 2009), and used custom scripts available at https://github.com/kpowder/Biology2022. Briefly, RAD markers were initially binned into linkage groups according to their position in the *M. zebra* UMD2a reference genome, cross referenced based on segregation patterns and recombination frequencies, and removed if located in unplaced scaffolds that had more than 40% of missing data or did not demonstrate linkage disequilibrium with multiple markers in a single linkage group. Additional manual curation was used to minimize the number of crossovers for those markers whose recombination frequency profile did not match their position in the linkage map, likely due to being within a misassembled region of the reference genome or a structural variant. The final genetic map included 22 linkage groups, 1267 total markers, 19-127 markers per linkage group, and was 1307.2 cM in total size.

Quantitative trait loci (QTL) analysis

QTL analysis used the R/qtl package (version 1.44-9) (Arends, Prins, Jansen, & Broman, 2010; Broman, Wu, Sen, & Churchill, 2003) following (Jansen, 1994). Scripts are described in (Powder, 2020) and available at https://github.com/kpowder/MiMB_QTL. A multiple-QTL mapping (MQM) approach was used to more accurately identify intervals and their effects (Jansen, 1994).The approach starts by using the onescan function in R/qtl (Broman, 2009) to identify putative, unlinked QTL. These putative QTL were used as cofactors to build a statistical model, and were verified by backward elimination to generate the final model. Statistical significance was assessed using 1000 permutations

to identify 5% (significant) and 10% (suggestive) cutoffs. For each of these QTL peaks, 95% confidence intervals on each linkage group were identified by Bayes analysis. Table S1 includes for each trait the cofactors used to build models, significance cutoffs, confidence intervals, and allelic effects at the peak marker of the QTL interval.

Identification of candidate genes

Markers are named based on physical locations (contig and nucleotide position) in the *Metriaclima zebra* UMD2a reference genome. These nucleotide positions were used in the NCBI genome data viewer (https://www.ncbi.nlm.nih.gov/genome/gdv, *M. zebra* annotation release 104) to retrieve candidate Entrez gene IDs and genomic locations. If the extremes of the 95% confidence interval included markers that mapped to unplaced scaffolds, the closest marker that mapped to a placed scaffold was used as an alternative. Full gene names were extracted from the Database for Visualization and Integrated Discovery (DAVID) (Huang , Sherman, & Lempicki, 2009; Huang, Sherman, & Lempicki, 2009) using Entrez gene ID numbers as a query. Genes previously associated with body pigmentation or melanocyte development were extracted from the annotated Molecular Signatures Database (Liberzon et al., 2011), which is used for Gene Set Enrichment Analysis (Subramanian et al., 2005). A total of 258 genes from the human data set were used, which associated with the gene ontology (GO) cellular component term pigment granule (GO:0048770) and the following biological process terms: cellular pigmentation (GO:0033059), developmental pigmentation (GO:0048066), establishment of pigment granule localization (GO:0051905), melanocyte differentiation (GO:0030318), melanocyte proliferation (GO:0097325), melanosome assembly (GO:1903232), pigment

accumulation (GO:0043476), pigment biosynthetic process (GO:0046148), pigment catabolic process (GO:0046149), pigment cell differentiation (GO:0050931), pigment granule localization (GO:0051875), pigment granule maturation (GO:0048757), pigment granule organization (GO:0048753), pigment metabolic process (GO:0042440), pigmentation (GO:0043473), positive regulation of developmental pigmentation (GO:0048087), positive regulation of melanocyte differentiation (GO:0045636), regulation of melanocyte differentiation (GO:0045634), regulation of pigment cell differentiation (GO:0050932), and regulation of pigmentation (GO:0120305).

RESULTS

Phenotypic variation in barring

We sought to examine the genetic factors that control variation in vertical bars across the flank, particularly the levels of eumelanin produced by melanophores and the spacing of bars and interbars. To accomplish this, we generated a hybrid cross between two species with distinct barring patterns. Importantly, given that both parents demonstrate some degree of barring, this cross is unlikely to identify genomic regions that are master regulators of bars (i.e., presence versus absence of bars), but rather how bars can be modified when they are present.

Aulonocara koningsi are distinguished by a regular series of vertical, melanic bars that extend on the anterior-posterior axis from the opercle to the caudal peduncle, and throughout the dorsal-ventral axis (Figure 1a). Melanic bars in *Aulonocara koningsi* are broken up by pale, lightly pigmented interbars that tend be narrower or the same width

as melanic bars (Figure 1a). Alternatively, *Metriaclima mbenjii* have vertical bars that typically occur on the flank only between the opercle and anal fin, then become more irregular or stop towards the posterior of the animal (Figure 1b). Interbars on *Metriaclima mbenjii* are more melanic, such that the overall effect of barring in this species is a subtle vertical bar on a dark background (Figure 1b). In agreement with these qualitative observations, quantification of the level of melanic pigmentation reveals that compared to *Metriaclima mbenjii,* black or brown pigment in *Aulonocara koningsi* is not significantly darker (Figure 2a) but can be significantly lighter (Figure 2b). This generates a significantly larger range of pigment (Figure 2c) and larger differences between pigment levels in bars and interbars (Figure 2g).

Though they have a visual difference in barring patterns, we did not find that parental species were significantly different in their patterns of vertical bars (Figure 2h-j). The exception to this is that *Metriaclima mbenjii* had significantly wider interbars (Figure 2k), though this is likely driven by the fact that the posterior of the flank in this species often did not have distinct bars, and due to a single specimen that had only a single bar and nearly the whole length of the body was classified as an interbar. We expect two factors explain the lack of statistical significance for most of the traits examined between the parental species. First, *Metriaclima mbenjii* is noted for a high percentage of ‘orange blotch’ (OB) animals, where melanophores are organized in irregular patches rather than bars. After removing these animals from the data set in order to focus on barring phenotypes, this only left six *Metriaclima mbenjii* parental specimens, reducing our statistical power. Second, our analysis that classified bars and interbars can have errors

in classification for an animal in which the grayscale intensity has less range and more inconsistent fluctuations, which was observed in many of the *Metriaclima mbenjii* parentals (i.e., compare pattern of the graph in Figure 1a versus variation around the average value in Figure 1b). An inability to accurately define bars and interbars in *Metriaclima mbenjii* parentals would influence measures of the average intensity of bars, the average intensity of interbars, the differential intensity between bars and interbars, the number of bars, the percent of barring, the average width of bars, and the average width of interbars, most of which did not show significant differences between parentals (Figure 2e-k).

Despite this, it's important to note that 100% of the 322 F_2 hybrids demonstrated a distinct barring pattern, resembling the *Aulonocara koningsi* parental phenotype, and thus would be classified correctly by our analysis approach. The dominance of this overall barring pattern observed in the *Aulonocara* x *Metriaclima* F_2 hybrids agrees with a previous suggestion that several genes are sufficient to drive the formation of bars (Gerwin et al., 2021). Though they all had melanic vertical bars, F_2 hybrids were phenotypically varied in terms of the level of eumelanin produced in the bars and interbars, as well as the spacing of these pigment elements. This population therefore can yield valuable insights into the patterns of phenotypic variation in barring, as well as the genetic loci that regulate this.

Color differences between males and females is thought to be sexually-selected, resulting in widespread sexual dimorphism across vertebrates (Bell & Zamudio, 2012; Hubbard et

al., 2010; Miller, Mesnick, & Wiens, 2021; Williams & Carroll, 2009), including cichlids (Brzozowski, Roscoe, Parsons, & Albertson, 2012; Konings, 2016; Salzburger, 2009; Santos et al., 2023). Within this cross however, we find no statistical relationship between any measures of pigment level or patterns and sex ($p = 0.24$ to 0.89, Table S2), nothing that F_2 animals were collected as juveniles and did not express fully mature nuptial coloration. Thus, variation identified here reflects differences due to species-specific genetic polymorphisms. Notably, within Lake Malawi cichlids, a set of ancestral polymorphisms are being recombined in differing combinations among species (Brawand et al., 2014; Malinsky et al., 2018; Svardal et al., 2020). Thus, even for traits with non-significant differences between parental species, QTL mapping can identify genetic factors that underlie pigment variation within this radiation and genetic combinations that are possible in other species.

Genetic basis of variation in pigment phenotypes

To determine the genetic basis of variation in barring phenotypes, we genetically mapped seven traits related to the level of eumelanin produced and four traits related to the location of bars. Fifty-one QTL underlie quantitative differences in pigmentation in *Metriaclima* x *Aulonocara* F_2 hybrids, with 48 that reach 5% statistical significance at the genome-wide level (Figure 3, Figure S2, Figure S3, and Table S1). An additional 3 QTL are suggestive at the 10% level and included in supplemental material only (Figure S2, Figure S3, and Table S1). QTL are found on 17 of 22 linkage groups, with each linkage group containing 1-6 significant loci each.

Between one and six QTL contribute to each trait, with each interval explaining 4.75-16.1% of variation for each trait (average 7.25% variation explained, Figure S3 and Table S1). While these data indicate that all these pigment traits are multifactorial, the QTL identified cumulatively explain a considerable portion of variation for multiple traits. Five QTL together explain 42.66% of variation in the number of bars, eight QTL explain 44.07% of variation in the average intensity of bars, seven QTL combine to explain 50.61% of variation in lightest intensity, and eight QTL cumulatively explain 69.14% of the total variation in covariance, or the discrepancy between dark bars on a lightly pigmented flank.

There is a large degree of overlap in our QTL intervals, which is expected given both the traits analyzed and their degree of correlation. For example, LG9 contains three QTL that overlap between 20.7-56.0 cM and control the lightness intensity, range of intensity, and average intensity of bars (Figure 3 and Table S1). A change in lightness would directly affect the calculation of the range of intensity, explaining why these traits map to the same interval. Accordingly, these traits are highly correlated ($r = 0.90$, Table S3) and the lightest intensity is also correlated with the average intensity of bars ($r = 0.87$, Table S3). These types of phenotypic correlations also explain the overlapping QTL on LG15 from 26.0-30.5 cM for lightest intensity, average intensity of bars, and average intensity of interbars (Figure 3 and Table S1), traits that all correlate ($r = 0.87$ to 0.96, Table S3). However, it's important to note that even highly correlated traits can be regulated through distinct mechanisms (i.e., many-to-one mapping (Wainwright, Alfaro, Bolnick, & Hulsey, 2005)). For example, darkest intensity, average intensity of bars, and average intensity of interbars are all highly correlated ($0.84 < r < 0.95$, Table S3). Together, these traits map

373 to fourteen intervals, ten of which are unique genomic regions. Further, five of the eight
374 QTL for the average intensity of bars are on LGs that do not contain any QTL for the other
375 two correlated traits.
376
377 The effect of specific alleles on phenotypes is varied across phenotypes (Figure S3 and
378 Table S1). For instance, for the QTL on LG12, the allele inherited from the *Metriaclima*
379 *mbenjii* granddam decreases the number of bars on LG12, but increases the number of
380 bars on LG13. Three other examples highlight the complex genetic interactions that are
381 possible within these species and across the cichlid radiation. First are the set of
382 overlapping QTL on LG9 and cluster of QTL on LG22. In both cases, alleles inherited
383 from *Metriaclima mbenjii* are associated with lighter intensity values (Figure S3 and Table
384 S1), though lighter pigmentation is associated with the *Aulonocara koningsi* phenotype
385 (Figure 1-b and Figure 2b). The second example is a group of QTL related to pigmentation
386 levels that occur on LG15. All 5 QTL demonstrate an underdominant inheritance pattern,
387 such that a combination of heterozygous alleles explain the variation in lightest intensity,
388 range of intensity, covariance, average intensity of bars, and average intensity of interbars
389 (Figure S3 and Table S1). These suggest that complex interactions between genes (i.e.,
390 epistasis (Carlborg & Haley, 2004; Phillips, 2008)) regulate these phenotypic traits such
391 that the effects of the *Metriaclima mbenjii* allele are only visible in the absence of or in
392 combination with additional alleles. These examples of cryptic genetic variation (Gibson
393 & Dworkin, 2004; Paaby & Rockman, 2014) are important to understand the full spectrum
394 of genetic factors that regulate a complex trait like pigmentation, and allelic combinations

that are likely to be present in other cichlid species within Lake Malawi (Brawand et al., 2014; Malinsky et al., 2018; Svardal et al., 2020).

Distinct genetic origins underlie pigment levels and patterning

We hypothesized that a separate set of genetic, molecular, and developmental mechanisms may underlie variation in the level of melanic pigmentation and the patterns of vertical bars. That is, we predicted that one set of genes would control where melanophores would be located and capable of generating dark vertical bars (i.e., patterning), and a separate set of genes would then control how much eumelanin is produced by these melanophores (i.e., pigment level). One set of data supporting this is an analysis of correlations among traits (Table S3). While some measures of pigment levels are correlated as discussed above, none of the four measures related to patterning were correlated with any of the seven measures of pigment level (r = -0.39 to 0.31 in pairwise comparisons, Table S3).

QTL data also largely supports that divergent genetic factors regulate pigment intensity and bar/interbar locations, through the examination of the degree of overlap of QTL intervals (Figure 3). We found numerous overlaps within similar types of traits. That is, LG5 and LG12 contain regions that have 2-3 overlapping QTL related to patterning, and LG8-24, LG9, LG15, LG18, and LG22 have 2-4 QTL at the same genomic locus that control levels of pigment produced.

Only LG4, LG13, LG14, and LG20 have overlapping 95% confidence intervals for traits related to pigment level and patterning, and additional examination of these regions suggest that a pleiotropic effect on both aspects of pigmentation is limited to LG13 and LG20 (Figure 4). For instance, all four QTL on LG4 have 95% confidence intervals that overlaps from 0-5.79 cM (Figure 3 and Table S1). However, this includes the peak and full region for the three traits related to pigment level, while the QTL for patterning has a peak at 20 cM and dips below significance under the peak of the other QTL, suggesting that two linked, but distinct loci may underlie variation in the two traits (Figure 4). Another overlap occurs on LG14, where a QTL for the differential intensity between bars and interbars overlaps with a QTL for the number of bars from 14.6-17.32 cM (Figure 3 and Table S1). However, closer examination of these loci reveals that the peak for these QTL are on opposite ends of the linkage group, 55 cM apart (Figure 4), and this overlapping interval is unlikely to contain a causative gene that underlies both the pigment level phenotype and the patterning phenotype.

However, two regions may regulate both pigment intensity and location on the body. First is on LG20, where a QTL for differential intensity between bars and interbars resides within QTL for number of bars and average width of bars (Figure 3). While the peak for the patterning QTL are both at 35 cM and the peak for the pigment level QTL is at 45 cM, these three all feature broad peaks with a high degree of overlap (Figure 4 and Table S1). Finally, six separate QTL reside on LG13 and span the entirety of the chromosome (Figure 3). Examination of the peaks and confidence intervals (Figures 3-4 and Table S1) suggests that at least 3 separate regions of LG13 are contributing to the pigment traits

440 measured. This includes a region from 0-11.37 cM containing a QTL for lightest intensity,
441 a region from 26.11-36.24 cM with a QTL for covariance, and a region from 42.85-48.33
442 cM that includes a QTL for darkest intensity (Figures 3-4). These three QTL do not overlap
443 each other, but the latter two both overlap QTL for average intensity of bars, number of
444 bars, and average width of bar (Figures 3-4). Thus, in the case of both LG13 and LG20,
445 more detailed mapping will be necessary to determine if these traits are regulated by the
446 same gene, distinct genes that are in close physical distance or linkage with each other,
447 or distinct genomic loci.
448
449 **DISCUSSION**
450 Though it is one of the most common pigment patterns in fishes, we know relatively little
451 about the genetic basis of dark vertical barring (Santos et al., 2023). To address this, we
452 used a genetic mapping cross between two cichlids with distinct presentations of barring
453 and mapped 48 genetic loci that influence the relative levels of melanic pigment in bars
454 and interbars, as well as their patterning. In addition to identifying this series of
455 quantitative trait loci, we found eumelanin pigment levels and barring patterns are largely
456 regulated by independent loci. These separate, polygenic genetic architectures would
457 enable evolutionary fine-tuning of barring in response to natural or sexual selection,
458 promoting further diversity in pigmentation. Further, we observed that vertical barring is
459 not due to a master regulatory gene, but a combination of genetic factors. This directly
460 contrasts with two other traits with distinct arrangements of melanophores, horizontal
461 stripes and blotching, controlled by *agouti-related protein 2* (*agrp2*) and *paired box 7a*

462 (*pax7a*), respectively (Kratochwil et al., 2018; Roberts et al., 2009). Our data thus
463 supports a previous suggestion that barring in cichlids is polygenic (Gerwin et al., 2021).
464
465 Our loci add to a variety of genetic factors of both small and large effect that regulate
466 pigmentation in cichlids (Albertson et al., 2014; Kratochwil et al., 2018). These alleles for
467 fin pigmentation (Ahi & Sefc, 2017; Albertson et al., 2014; Salzburger et al., 2007; Santos
468 et al., 2014), xanthophore-based red and yellow coloration (Albertson et al., 2014; Wang
469 et al., 2022), melanophore-based black and brown coloration (Albertson et al., 2014;
470 Kratochwil et al., 2018; Roberts et al., 2009), and integration versus modularity of color
471 patterns across the flank (Albertson et al., 2014) are shuffled in differing combinations
472 (Brawand et al., 2014; Malinsky et al., 2018; Svardal et al., 2020) to generate the range
473 of colors and patterns that characterize the adaptive radiation of cichlids (Kocher, 2004;
474 Konings, 2016; Santos et al., 2023). These pigmentation patterns, whether inherited
475 independently or not, are then subject to a variety of ecologically-relevant selective
476 pressures such as predator avoidance and intrasexual competitive interactions (Brandon
477 et al., 2023; Cuthill et al., 2017; Eizirik & Trindade, 2021; Hubbard et al., 2010; Korzan &
478 Fernald, 2007; Maan & Sefc, 2013; Parichy, 2021; Protas & Patel, 2008; Sefc et al., 2014).
479 One critical implication of these hues and patterns is assortative mating (Couldrige &
480 Alexander, 2002; Jordan, Kellogg, Juanes, & Stauffer, 2003), which can directly result in
481 reproductive isolation, and thus sexual selection has been central to the dramatic
482 speciation and divergence of cichlids (Danley & Kocher, 2001; Muschick et al., 2014;
483 Ronco et al., 2021; Wagner et al., 2012).
484

The majority of our QTL do not include a series of genes previously associated with variation in pigment (Figure 3) in cichlids (Albertson et al., 2014; Kratochwil et al., 2018; Kratochwil et al., 2019; Roberts et al., 2009; Salzburger et al., 2007; Santos et al., 2014; Wang et al., 2022), *Danio* species including those with vertical barring (Lamason et al., 2005; Mills, Nuckels, & Parichy, 2007; Parichy et al., 2000; Parichy, Rawls, Pratt, Whitfield, & Johnson, 1999; Parichy & Turner, 2003; Podobnik et al., 2020), cavefish (Gross, Borowsky, & Tabin, 2009; Protas et al., 2006), sticklebacks (Greenwood, Cech, & Peichel, 2012), and other non-fish vertebrates (Domyan et al., 2014; Hoekstra, 2006; Jablonski, 2021; Lamason et al., 2005; Lu et al., 2016; Mallarino et al., 2016). For instance, *melanocortin 1 receptor* (*mc1r*) on LG1 has been associated with a series of adaptive pigment changes, through regulation of the biosynthesis of eumelanin (Hoekstra, 2006). While activating or repressing eumelanin production would likely influence any of the seven traits related to pigment level that we measured, none of the 35 QTL that underlie these traits include *mc1r*. Additional work will be needed to narrow genetic intervals, verify candidate genes, and identify the molecular and cellular mechanisms that generate the phenotypes we mapped. Most of our genetic intervals contain many genes, from 40 genes for covariance on LG10 to the entire chromosome and 1069 genes for the average intensity of interbars on LG18 (average = 342 genes, Table S4). However, we discuss below a number of strong candidate genes within these intervals and how they may mediate variation in melanic traits.

One set of candidate genes are associated with the development and survival of the melanophores themselves, including trunk neural crest cells which are the embryonic

source of these pigment cells (Brandon et al., 2023; Parichy, 2021). Variation in the induction, migration, and differentiation process could change the number and/or location of melanophores present within the skin to generate changes in both the pattern of barring and the intensity of melanin produced. For instance, a QTL for average width of bars on LG4 includes the candidate gene *SRY-box 10* (*sox10*). We note that *sox10* is near, but not included in QTL for the lightest intensity, average intensity of bars, and differential intensity between bars and interbars that partially overlap this QTL for average width of bars (Figure 3 and Table S1). *Sox10* is necessary for neural crest cell specification (Carney et al., 2006; Jacob, 2015) and required to establish the melanophore linage (Marathe et al., 2017). Genetic variation in this gene in humans results in Waardenburg syndrome, which is characterized by a suite of alterations to neural crest cell derivatives, one of which is depigmented patches in the skin and hair (Pingault et al., 2010; Pingault, Zerad, Bertani-Torres, & Bondurand, 2022). This is not the only candidate gene associated with a pigmentation condition in humans. Overlapping QTL on LG13 contribute to covariance, the number of bars, and the average width of bars (Figure 3). These three QTL all include the candidate gene *F-box protein 11a* (*fbxo11a*) and the QTL for number of bars and average width of bars also include *SPARC-related modular calcium binding 2* (*smoc2*) (Table S4). Both genes are associated with the human condition vitiligo, characterized by the progressive loss of pigment cells through cell death or autoimmunity (Alkhateeb, Al-Dain Marzouka, & Qarqaz, 2010; Birlea, Gowan, Fain, & Spritz, 2010; Le Poole et al., 2001; Xie et al., 2016). Though little is known about the molecular function of *smoc2*, *fbxo11* regulates melanocyte proliferation, apoptosis, and intracellular transport of the eumelanin biosynthesis enzyme tyrosinase (Guan et al.,

2010). Such a loss of melanophores in localized regions could result in the changes in barring pattern or amount of melanin produced and counting of individual melanophores (O'Quin et al., 2013; O'Quin et al., 2012) may provide further insights into this regulation.

The location and number of melanocytes would also be impacted by genes that regulate fate decisions during melanophore development. The QTL for covariance on LG5 includes the gene *pax7a*, and a related gene, *paired box 3b* (*pax3b*), is located within a QTL on LG14 for differential intensity of bars and interbars. *Pax3a*, the paralog of our candidate, and *pax7a* and can act transcriptionally as switch factors between different pigment cell fates, and these genes have previously been associated in cichlids with changes in the balance of melanophore and xanthophore cell numbers, changes in pigment levels, or altered patterns such as melanic blotches (Albertson et al., 2014; Minchin & Hughes, 2008; Roberts et al., 2017; Roberts et al., 2009). An overlapping QTL for the lightest intensity and the average intensity of interbars on LG18 includes another candidate gene related to cell fate decisions. *Endothelin receptor type B* (*ednrb*) is required for differentiation of melanophores (Saldana-Caboverde & Kos, 2010) and another pigment cell in fishes, iridophores (Krauss et al., 2014). Mutations in *ednrb* result in broken stripes in zebrafish (Parichy et al., 2000), though it has yet to be determined if the spots caused by this fate switch could merge into a bar pattern instead of stripes. Also within this interval on LG18 is the master switch for horizontal stripes in cichlids, *agrp2* (Figure 3). Previous work has predicted that stripes and bars are regulated by genetically-independent modules (Gerwin et al., 2021), suggesting that *agrp2* is not the causative gene on LG18 for changes in our bar phenotypes. However, it is possible that this

554 independence depends on the cichlid species being compared, and *agrp2* may regulate
555 barring in *Metriaclima* and *Aulonocara*.
556
557 Once melanophores are specified and migrate to their position on the flank, variation in
558 eumelanin biosynthesis can produce variation. This would be expected to change
559 pigment intensity, but not the pattern of barring. In agreement with this, the three QTL
560 intervals described below that contain candidate genes associated with eumelanin
561 production are associated with at least one of the measures of pigment level, but none of
562 the measures of bar location. The LG5 QTL for covariance and the LG10 QTL for average
563 intensity of bars contain two genes that have been associated with the biosynthesis of
564 melanin across multiple vertebrate species, *agouti signaling protein* (*asip*) and *tyrosinase*
565 (*tyr*) (Hoekstra, 2006). Interestingly, *asip* is also associated with countershading, a
566 dorsoventral gradient of pigmentation important for predator avoidance, the switch
567 between production of dark eumelanin and yellow/red pheomelanin, and may also
568 repress melanophore differentiation (Cal et al., 2019; Ceinos, Guillot, Kelsh, Cerda-
569 Reverter, & Rotllant, 2015; Steiner, Rompler, Boettger, Schoneberg, & Hoekstra, 2009).
570 Candidate genes may also regulate melanin production based on ecological triggers. For
571 instance, within the LG15 QTL associated with lightest intensity, covariance, average
572 intensity of bars, and average intensity of interbars is the candidate gene *melanocortin 2*
573 *receptor accessory protein 2* (*mrpa2*). This gene is involved in the melanocortin response
574 pathway, and can modulate melanin levels following starvation- or crowding-induced
575 stress (Cortes et al., 2014).
576

Finally, variation in barring can be generated by differences in pigment density and distribution or alteration of melanophore cell density and shape (Liang, Gerwin, Meyer, & Kratochwil, 2020). While this can be rapidly regulated in cichlids through physiological changes such as hormone signaling (Muske & Fernald, 1987; O'Quin et al., 2012), this can also be regulated at the genetic level. Within the overlapping regions on LG4 for QTL regulating lightest intensity, average intensity of bars, and differential intensity between bars and interbars is *melanin-concentrating hormone receptor 1b* (*mchr1b*). This G-protein coupled receptor integrates with the nervous system to regulate hormonal changes in pigment aggregation as a fish alters its pigmentation for camouflage from predators, to attract a mate, or in response to intrasexual competition (Madelaine, Ngo, Skariah, & Mourrain, 2020; Mizusawa et al., 2011). Another strong candidate gene is found within a QTL on LG14 for differential intensity between bars and interbars. *Potassium inwardly rectifying channel subfamily J member 13* (*kcnj13*) is necessary for interactions between melanophores and other pigment cell types such as iridophores and xanthophores, resulting in localized changes in chromatophore shape and changes in the contrast of pigment patterns (Podobnik et al., 2022). Notably, *kcnj13* is associated with the evolution of vertical barring in *Danio* species, suggesting a conserved role in barring across a large portion of the fish phylogeny (Podobnik et al., 2020). Finally, a QTL for the number of bars on LG20 includes the gene *premelanosome protein b* (*pmelb*). *Pmelb* encodes a protein specific to pigment cells, that affects the cellular structure and shape of melanosomes through formation of fibrillar sheets on which melanin polymerizes and is deposited (Hellstrom et al., 2011; Schonthaler et al., 2005; Watt, van Niel, Raposo, & Marks, 2013). Further, CRISPR inactivation of paralogs *pmela* and *pmelb* in tilapia

600 resulted in a reduction of melanophore number and size, as well as a loss of a vertical
601 barring pattern (Wang et al., 2022).
602
603 **CONCLUSIONS**
604 Pigment hues and patterns can be selected by a series of natural and sexual selective
605 pressures including predator avoidance, mate choice, and competitive interactions. Here
606 we explore one common pattern with the diverse coloration found in cichlid fishes, vertical
607 melanic barring, for which the genetic and molecular basis is largely unexplored. We show
608 here that the genomic intervals that influence pigment levels are largely distinct from
609 those that regulate bar patterning, which can promote the degree of variation that is
610 possible in this trait. A series of candidate genes within these intervals highlight the varied
611 ways that melanophore development can be altered to produce ecologically-relevant
612 variation in barring. The pigmentation patterns studied here are particularly important for
613 the adaptive radiation of cichlids, where they play a role in sexual selection and
614 reproductive isolation, and therefore in maintaining species boundaries. Future studies
615 identifying the causative alleles for the QTL we identify here will allow exploration of their
616 evolutionary history across the cichlid radiation, and their potential role in speciation.
617
618 **ACKNOWLEDGEMENTS**
619 This work was supported by NSF CAREER IOS-1942178 (KEP), NIH P20GM121342
620 (KEP), NSF IOS-1456765 (RBR), and an Arnold and Mabel Beckman Institute Young
621 Investigator Award (RBR). This work is dedicated to the memory of Dr. Stephen L.

Johnson, who first introduced KEP to the beauty found in fish melanophores, and whose work helped inspire RBR to enter the world of fish genetics.

REFERENCES

Ahi, E. P., & Sefc, K. M. (2017). A gene expression study of dorso-ventrally restricted pigment pattern in adult fins of Neolamprologus meeli, an African cichlid species. *PeerJ, 5*, e2843. doi:10.7717/peerj.2843

Albertson, R. C., Powder, K. E., Hu, Y., Coyle, K. P., Roberts, R. B., & Parsons, K. J. (2014). Genetic basis of continuous variation in the levels and modular inheritance of pigmentation in cichlid fishes. *Mol Ecol, 23*(21), 5135-5150. doi:10.1111/mec.12900

Alkhateeb, A., Al-Dain Marzouka, N., & Qarqaz, F. (2010). SMOC2 gene variant and the risk of vitiligo in Jordanian Arabs. *Eur J Dermatol, 20*(6), 701-704. doi:10.1684/ejd.2010.1095

Arends, D., Prins, P., Jansen, R. C., & Broman, K. W. (2010). R/qtl: high-throughput multiple QTL mapping. *Bioinformatics, 26*(23), 2990-2992. doi:10.1093/bioinformatics/btq565

Bell, R. C., & Zamudio, K. R. (2012). Sexual dichromatism in frogs: natural selection, sexual selection and unexpected diversity. *Proc Biol Sci, 279*(1748), 4687-4693. doi:10.1098/rspb.2012.1609

Birlea, S. A., Gowan, K., Fain, P. R., & Spritz, R. A. (2010). Genome-wide association study of generalized vitiligo in an isolated European founder population identifies SMOC2, in close proximity to IDDM8. *J Invest Dermatol, 130*(3), 798-803. doi:10.1038/jid.2009.347

Brandon, A. A., Almeida, D., & Powder, K. E. (2023). Neural crest cells as a source of microevolutionary variation. *Seminars Cell & Dev Biol, 145*, 42-51.

Brawand, D., Wagner, C. E., Li, Y. I., Malinsky, M., Keller, I., Fan, S., . . . Di Palma, F. (2014). The genomic substrate for adaptive radiation in African cichlid fish. *Nature, 513*(7518), 375-381. doi:10.1038/nature13726

Broman, K. W. (2009). *A guide to QTL mapping with R/qtl*. New York, NY: Springer.

Broman, K. W., Wu, H., Sen, S., & Churchill, G. A. (2003). R/qtl: QTL mapping in experimental crosses. *Bioinformatics, 19*(7), 889-890. doi:10.1093/bioinformatics/btg112

Brzozowski, F., Roscoe, J., Parsons, K., & Albertson, C. (2012). Sexually dimorphic levels of color trait integration and the resolution of sexual conflict in Lake Malawi cichlids. *J Exp Zool B Mol Dev Evol, 318*(4), 268-278. doi:10.1002/jez.b.22443

Cal, L., Suarez-Bregua, P., Comesana, P., Owen, J., Braasch, I., Kelsh, R., . . . Rotllant, J. (2019). Countershading in zebrafish results from an Asip1 controlled dorsoventral gradient of pigment cell differentiation. *Sci Rep, 9*(1), 3449. doi:10.1038/s41598-019-40251-z

Carlborg, O., & Haley, C. S. (2004). Epistasis: too often neglected in complex trait studies? *Nat Rev Genet, 5*(8), 618-625. doi:10.1038/nrg1407

664 Carney, T. J., Dutton, K. A., Greenhill, E., Delfino-Machin, M., Dufourcq, P., Blader, P., &
665 Kelsh, R. N. (2006). A direct role for Sox10 in specification of neural crest-derived
666 sensory neurons. *Development, 133*(23), 4619-4630. doi:10.1242/dev.02668
667 Castle, W. E., & Allen, G. M. (1903). The Heredity of Albinism. *Proc Am Acad Arts Sci,*
668 *38*(21), 603-622.
669 Ceinos, R. M., Guillot, R., Kelsh, R. N., Cerda-Reverter, J. M., & Rotllant, J. (2015).
670 Pigment patterns in adult fish result from superimposition of two largely
671 independent pigmentation mechanisms. *Pigment Cell Melanoma Res, 28*(2), 196-
672 209. doi:10.1111/pcmr.12335
673 Cortes, R., Agulleiro, M. J., Navarro, S., Guillot, R., Sanchez, E., & Cerda-Reverter, J. M.
674 (2014). Melanocortin receptor accessory protein 2 (MRAP2) interplays with the
675 zebrafish melanocortin 1 receptor (MC1R) but has no effect on its pharmacological
676 profile. *Gen Comp Endocrin, 201*, 30-36.
677 Couldrige, V. C. K., & Alexander, G. J. (2002). Color patterns and species recognition in
678 four closely related species of Lake Malawi cichlid. *Behav Ecol, 18*, 59-64.
679 Cuthill, I. C., Allen, W. L., Arbuckle, K., Caspers, B., Chaplin, G., Hauber, M. E., . . . Caro,
680 T. (2017). The biology of color. *Science, 357*(6350). doi:10.1126/science.aan0221
681 Danley, P. D., & Kocher, T. D. (2001). Speciation in rapidly diverging systems: lessons
682 from Lake Malawi. *Mol Ecol, 10*(5), 1075-1086. doi:10.1046/j.1365-
683 294x.2001.01283.x
684 Darwin, C. (1871). *The Descent of Man, and Selection in Relation to Sex*: John Murray.
685 DeLorenzo, L., Mathews, D., Brandon, A. A., Joglekar, M., Carmona Baez, A., Moore, E.
686 C., . . . Powder, K. E. (2023). Genetic basis of ecologically relevant body shape
687 variation among four genera of cichlid fishes. *Mol Ecol*. doi:10.1111/mec.16977
688 Domyan, E. T., Guernsey, M. W., Kronenberg, Z., Krishnan, S., Boissy, R. E., Vickrey, A.
689 I., . . . Shapiro, M. D. (2014). Epistatic and combinatorial effects of pigmentary
690 gene mutations in the domestic pigeon. *Curr Biol, 24*(4), 459-464.
691 doi:10.1016/j.cub.2014.01.020
692 Eizirik, E., & Trindade, F. J. (2021). Genetics and Evolution of Mammalian Coat
693 Pigmentation. *Annu Rev Anim Biosci, 9*, 125-148. doi:10.1146/annurev-animal-
694 022114-110847
695 Gerwin, J., Urban, S., Meyer, A., & Kratochwil, C. F. (2021). Of bars and stripes: A Malawi
696 cichlid hybrid cross provides insights into genetic modularity and evolution of
697 modifier loci underlying colour pattern diversification. *Mol Ecol, 30*(19), 4789-4803.
698 doi:10.1111/mec.16097
699 Gibson, G., & Dworkin, I. (2004). Uncovering cryptic genetic variation. *Nat Rev Genet,*
700 *5*(9), 681-690. doi:10.1038/nrg1426
701 Greenwood, A. K., Cech, J. N., & Peichel, C. L. (2012). Molecular and developmental
702 contributions to divergent pigment patterns in marine and freshwater sticklebacks.
703 *Evol Dev, 14*(4), 351-362. doi:10.1111/j.1525-142X.2012.00553.x
704 Greenwood, A. K., Jones, F. C., Chan, Y. F., Brady, S. D., Absher, D. M., Grimwood, J.,
705 . . . Peichel, C. L. (2011). The genetic basis of divergent pigment patterns in
706 juvenile threespine sticklebacks. *Heredity (Edinb), 107*(2), 155-166.
707 doi:10.1038/hdy.2011.1

708 Gross, J. B., Borowsky, R., & Tabin, C. J. (2009). A novel role for Mc1r in the parallel
709 evolution of depigmentation in independent populations of the cavefish Astyanax
710 mexicanus. *PLoS Genet, 5*(1), e1000326. doi:10.1371/journal.pgen.1000326
711 Guan, C., Lin, F., Zhou, M., Hong, W., Fu, L., Xu, W., . . . Xu, A. (2010). The role of
712 VIT1/FBXO11 in the regulation of apoptosis and tyrosinase export from
713 endoplasmic reticulum in cultured melanocytes. *Int J Mol Med, 26*(1), 57-65.
714 doi:10.3892/ijmm_00000435
715 Hellstrom, A. R., Watt, B., Fard, S. S., Tenza, D., Mannstrom, P., Narfstrom, K., . . .
716 Andersson, L. (2011). Inactivation of Pmel alters melanosome shape but has only
717 a subtle effect on visible pigmentation. *PLoS Genet, 7*(9), e1002285.
718 doi:10.1371/journal.pgen.1002285
719 Hoekstra, H. E. (2006). Genetics, development and evolution of adaptive pigmentation in
720 vertebrates. *Heredity (Edinb), 97*(3), 222-234. doi:10.1038/sj.hdy.6800861
721 Huang , D. W., Sherman, B. T., & Lempicki, R. A. (2009). Bioinformatics enrichment tools:
722 paths toward the comprehensive functional analysis of large gene lists. *Nucleic*
723 *Acids Res, 37*(1), 1-13. doi:10.1093/nar/gkn923
724 Huang, D. W., Sherman, B. T., & Lempicki, R. A. (2009). Systematic and integrative
725 analysis of large gene lists using DAVID bioinformatics resources. *Nat Protoc, 4*(1),
726 44-57. doi:10.1038/nprot.2008.211
727 Hubbard, J. K., Uy, J. A., Hauber, M. E., Hoekstra, H. E., & Safran, R. J. (2010).
728 Vertebrate pigmentation: from underlying genes to adaptive function. *Trends*
729 *Genet, 26*(5), 231-239. doi:10.1016/j.tig.2010.02.002
730 Jablonski, N. G. (2021). The evolution of human skin pigmentation involved the
731 interactions of genetic, environmental, and cultural variables. *Pigment Cell*
732 *Melanoma Res, 34*(4), 707-729. doi:10.1111/pcmr.12976
733 Jacob, C. (2015). Transcriptional control of neural crest specification into peripheral glia.
734 *Glia, 63*(11), 1883-1896. doi:10.1002/glia.22816
735 Jansen, R. C. (1994). Controlling the type I and type II errors in mapping quantitative trait
736 loci. *Genetics, 138*(3), 871-881.
737 Jordan, R., Kellogg, K., Juanes, F., & Stauffer, J. (2003). Evaluation of female mate
738 choice cues in a group of Lake Malawi mbuna (Cichlidae). *Copeia, 2003*, 181-186.
739 Kocher, T. D. (2004). Adaptive evolution and explosive speciation: the cichlid fish model.
740 *Nat Rev Genet, 5*(4), 288-298. doi:10.1038/nrg1316
741 Konings, A. (2016). *Malawi cichlids in their natural habitat* (5th ed.): Cichlid Press.
742 Korzan, W. J., & Fernald, R. D. (2007). Territorial male color predicts agonistic behavior
743 of conspecifics in a color polymorphic species. *Behav Ecol, 18*, 318-323.
744 Kratochwil, C. F., Liang, Y., Gerwin, J., Woltering, J. M., Urban, S., Henning, F., . . .
745 Meyer, A. (2018). Agouti-related peptide 2 facilitates convergent evolution of stripe
746 patterns across cichlid fish radiations. *Science, 362*(6413), 457-460.
747 doi:10.1126/science.aao6809
748 Kratochwil, C. F., Urban, S., & Meyer, A. (2019). Genome of the Malawi golden cichlid
749 fish (Melanochromis auratus) reveals exon loss of oca2 in an amelanistic morph.
750 *Pigment Cell Melanoma Res, 32*(5), 719-723. doi:10.1111/pcmr.12799
751 Krauss, J., Frohnhofer, H. G., Walderich, B., Maischein, H. M., Weiler, C., Irion, U., &
752 Nusslein-Volhard, C. (2014). Endothelin signalling in iridophore development and

753 stripe pattern formation of zebrafish. *Biol Open, 3*(6), 503-509.
754 doi:10.1242/bio.20148441
755 Lamason, R. L., Mohideen, M. A., Mest, J. R., Wong, A. C., Norton, H. L., Aros, M. C., . .
756 . Cheng, K. C. (2005). SLC24A5, a putative cation exchanger, affects pigmentation
757 in zebrafish and humans. *Science, 310*(5755), 1782-1786.
758 doi:10.1126/science.1116238
759 Le Poole, I. C., Sarangarajan, R., Zhao, Y., Stennett, L. S., Brown, T. L., Sheth, P., . . .
760 Boissy, R. E. (2001). 'VIT1', a novel gene associated with vitiligo. *Pigment Cell*
761 *Res, 14*(6), 475-484. doi:10.1034/j.1600-0749.2001.140608.x
762 Liang, Y., Gerwin, J., Meyer, A., & Kratochwil, C. F. (2020). Developmental and Cellular
763 Basis of Vertical Bar Color Patterns in the East African Cichlid Fish Haplochromis
764 latifasciatus. *Front Cell Dev Biol, 8*, 62. doi:10.3389/fcell.2020.00062
765 Liberzon, A., Subramanian, A., Pinchback, R., Thorvaldsdottir, H., Tamayo, P., & Mesirov,
766 J. P. (2011). Molecular signatures database (MSigDB) 3.0. *Bioinformatics, 27*(12),
767 1739-1740. doi:10.1093/bioinformatics/btr260
768 Lu, M. D., Han, X. M., Ma, Y. F., Irwin, D. M., Gao, Y., Deng, J. K., . . . Zhang, Y. P.
769 (2016). Genetic variations associated with six-white-point coat pigmentation in
770 Diannan small-ear pigs. *Sci Rep, 6*, 27534. doi:10.1038/srep27534
771 Maan, M. E., & Sefc, K. M. (2013). Colour variation in cichlid fish: Developmental
772 mechanisms, selective pressures and evolutionary consequences. *Seminars Cell*
773 *& Dev Biol, 24*, 516-518.
774 Madelaine, R., Ngo, K. J., Skariah, G., & Mourrain, P. (2020). Genetic deciphering of the
775 antagonistic activities of the melanin-concentrating hormone and melanocortin
776 pathways in skin pigmentation. *PLoS Genet, 16*(12), e1009244.
777 doi:10.1371/journal.pgen.1009244
778 Malinsky, M., Svardal, H., Tyers, A. M., Miska, E. A., Genner, M. J., Turner, G. F., &
779 Durbin, R. (2018). Whole-genome sequences of Malawi cichlids reveal multiple
780 radiations interconnected by gene flow. *Nat Ecol Evol, 2*(12), 1940-1955.
781 doi:10.1038/s41559-018-0717-x
782 Mallarino, R., Henegar, C., Mirasierra, M., Manceau, M., Schradin, C., Vallejo, M., . . .
783 Hoekstra, H. E. (2016). Developmental mechanisms of stripe patterns in rodents.
784 *Nature, 539*(7630), 518-523. doi:10.1038/nature20109
785 Marathe, H. G., Watkins-Chow, D. E., Weider, M., Hoffmann, A., Mehta, G., Trivedi, A., .
786 . . de la Serna, I. L. (2017). BRG1 interacts with SOX10 to establish the melanocyte
787 lineage and to promote differentiation. *Nucleic Acids Res, 45*(11), 6442-6458.
788 doi:10.1093/nar/gkx259
789 Miller, E. C., Mesnick, S. L., & Wiens, J. J. (2021). Sexual Dichromatism Is Decoupled
790 from Diversification over Deep Time in Fishes. *Am Nat, 198*(2), 232-252.
791 doi:10.1086/715114
792 Mills, M. G., Nuckels, R. J., & Parichy, D. M. (2007). Deconstructing evolution of adult
793 phenotypes: genetic analyses of kit reveal homology and evolutionary novelty
794 during adult pigment pattern development of Danio fishes. *Development, 134*(6),
795 1081-1090. doi:10.1242/dev.02799
796 Minchin, J. E., & Hughes, S. M. (2008). Sequential actions of Pax3 and Pax7 drive
797 xanthophore development in zebrafish neural crest. *Dev Biol, 317*(2), 508-522.
798 doi:10.1016/j.ydbio.2008.02.058

Mizusawa, K., Kobayashi, Y., Sunuma, T., Asahida, T., Saito, Y., & Takahashi, A. (2011). Inhibiting roles of melanin-concentrating hormone for skin pigment dispersion in barfin flounder, Verasper moseri. *Gen Comp Endocrinol, 171*(1), 75-81. doi:10.1016/j.ygcen.2010.12.008

Muschick, M., Nosil, P., Roesti, M., Dittmann, M. T., Harmon, L., & Salzburger, W. (2014). Testing the stages model in the adaptive radiation of cichlid fishes in East African Lake Tanganyika. *Proc Biol Sci, 281*(1795). doi:10.1098/rspb.2014.0605

Muske, L. E., & Fernald, R. D. (1987). Control of a teleost social signal. II. Anatomical and physiological specializations of chromatophores. *J Comp Physiol A, 160*(1), 99-107. doi:10.1007/BF00613445

O'Quin, C. T., Drilea, A. C., Conte, M. A., & Kocher, T. D. (2013). Mapping of pigmentation QTL on an anchored genome assembly of the cichlid fish, Metriaclima zebra. *BMC Genomics, 14*, 287. doi:10.1186/1471-2164-14-287

O'Quin, C. T., Drilea, A. C., Roberts, R. B., & Kocher, T. D. (2012). A small number of genes underlie male pigmentation traits in Lake Malawi cichlid fishes. *J Exp Zool B Mol Dev Evol, 318*(3), 199-208. doi:10.1002/jez.b.22006

Paaby, A. B., & Rockman, M. V. (2014). Cryptic genetic variation: evolution's hidden substrate. *Nat Rev Genet, 15*(4), 247-258. doi:10.1038/nrg3688

Parichy, D. M. (2021). Evolution of pigment cells and patterns: recent insights from teleost fishes. *Curr Opin Genet Dev, 69*, 88-96. doi:10.1016/j.gde.2021.02.006

Parichy, D. M., Mellgren, E. M., Rawls, J. F., Lopes, S. S., Kelsh, R. N., & Johnson, S. L. (2000). Mutational analysis of endothelin receptor b1 (rose) during neural crest and pigment pattern development in the zebrafish Danio rerio. *Dev Biol, 227*(2), 294-306. doi:10.1006/dbio.2000.9899

Parichy, D. M., Rawls, J. F., Pratt, S. J., Whitfield, T. T., & Johnson, S. L. (1999). Zebrafish sparse corresponds to an orthologue of c-kit and is required for the morphogenesis of a subpopulation of melanocytes, but is not essential for hematopoiesis or primordial germ cell development. *Development, 126*(15), 3425-3436. doi:10.1242/dev.126.15.3425

Parichy, D. M., & Turner, J. M. (2003). Temporal and cellular requirements for Fms signaling during zebrafish adult pigment pattern development. *Development, 130*(5), 817-833. doi:10.1242/dev.00307

Peterson, E. N., Cline, M. E., Moore, E. C., Roberts, N. B., & Roberts, R. B. (2017). Genetic sex determination in Astatotilapia calliptera, a prototype species for the Lake Malawi cichlid radiation. *Naturwissenschaften, 104*(5-6), 41. doi:10.1007/s00114-017-1462-8

Phillips, P. C. (2008). Epistasis--the essential role of gene interactions in the structure and evolution of genetic systems. *Nat Rev Genet, 9*(11), 855-867. doi:10.1038/nrg2452

Pingault, V., Ente, D., Dastot-Le Moal, F., Goossens, M., Marlin, S., & Bondurand, N. (2010). Review and update of mutations causing Waardenburg syndrome. *Hum Mutat, 31*(4), 391-406. doi:10.1002/humu.21211

Pingault, V., Zerad, L., Bertani-Torres, W., & Bondurand, N. (2022). SOX10: 20 years of phenotypic plurality and current understanding of its developmental function. *J Med Genet, 59*(2), 105-114. doi:10.1136/jmedgenet-2021-108105

Podobnik, M., Frohnhofer, H. G., Dooley, C. M., Eskova, A., Nusslein-Volhard, C., & Irion, U. (2020). Evolution of the potassium channel gene Kcnj13 underlies colour pattern diversification in Danio fish. *Nat Commun, 11*(1), 6230. doi:10.1038/s41467-020-20021-6

Podobnik, M., Singh, A. P., Fu, Z., Dooley, C. M., Frohnhöfer, H. G., Firlej, M., . . . Irion, U. (2022). Cis-regulatory evolution of the potassium channel gene kcnj13 during pigment pattern diversification in Danio fish. *bioRxiv*, 2022.2012.2005.519077. doi:10.1101/2022.12.05.519077

Powder, K. E. (2020). QTL analysis in fishes. In X. M. Shi (Ed.), *eQTL Analysis*: Springer.

Powder, K. E., & Albertson, R. C. (2016). Cichlid fishes as a model to understand normal and clinical craniofacial variation. *Dev Biol, 415*(2), 338-346. doi:10.1016/j.ydbio.2015.12.018

Protas, M. E., Hersey, C., Kochanek, D., Zhou, Y., Wilkens, H., Jeffery, W. R., . . . Tabin, C. J. (2006). Genetic analysis of cavefish reveals molecular convergence in the evolution of albinism. *Nat Genet, 38*(1), 107-111. doi:10.1038/ng1700

Protas, M. E., & Patel, N. H. (2008). Evolution of coloration patterns. *Annu Rev Cell Dev Biol, 24*, 425-446. doi:10.1146/annurev.cellbio.24.110707.175302

Roberts, R. B., Moore, E. C., & Kocher, T. D. (2017). An allelic series at pax7a is associated with colour polymorphism diversity in Lake Malawi cichlid fish. *Mol Ecol, 26*(10), 2625-2639. doi:10.1111/mec.13975

Roberts, R. B., Ser, J. R., & Kocher, T. D. (2009). Sexual conflict resolved by invasion of a novel sex determiner in Lake Malawi cichlid fishes. *Science, 326*(5955), 998-1001. doi:10.1126/science.1174705

Ronco, F., Matschiner, M., Bohne, A., Boila, A., Buscher, H. H., El Taher, A., . . . Salzburger, W. (2021). Drivers and dynamics of a massive adaptive radiation in cichlid fishes. *Nature, 589*(7840), 76-81. doi:10.1038/s41586-020-2930-4

Saldana-Caboverde, A., & Kos, L. (2010). Roles of endothelin signaling in melanocyte development and melanoma. *Pigment Cell Melanoma Res, 23*(2), 160-170. doi:10.1111/j.1755-148X.2010.00678.x

Salzburger, W. (2009). The interaction of sexually and naturally selected traits in the adaptive radiations of cichlid fishes. *Mol Ecol, 18*(2), 169-185. doi:10.1111/j.1365-294X.2008.03981.x

Salzburger, W., Braasch, I., & Meyer, A. (2007). Adaptive sequence evolution in a color gene involved in the formation of the characteristic egg-dummies of male haplochromine cichlid fishes. *BMC Biol, 5*, 51. doi:10.1186/1741-7007-5-51

Santos, M. E., Braasch, I., Boileau, N., Meyer, B. S., Sauteur, L., Bohne, A., . . . Salzburger, W. (2014). The evolution of cichlid fish egg-spots is linked with a cis-regulatory change. *Nat Commun, 5*, 5149. doi:10.1038/ncomms6149

Santos, M. E., Lopes, J. F., & Kratochwil, C. F. (2023). East African cichlid fishes. *Evodevo, 14*(1), 1. doi:10.1186/s13227-022-00205-5

Schindelin, J., Arganda-Carreras, I., Frise, E., Kaynig, V., Longair, M., Pietzsch, T., . . . Cardona, A. (2012). Fiji: an open-source platform for biological-image analysis. *Nat Methods, 9*(7), 676-682. doi:10.1038/nmeth.2019

Schonthaler, H. B., Lampert, J. M., von Lintig, J., Schwarz, H., Geisler, R., & Neuhauss, S. C. (2005). A mutation in the silver gene leads to defects in melanosome

889 biogenesis and alterations in the visual system in the zebrafish mutant fading
890 vision. *Dev Biol, 284*(2), 421-436. doi:10.1016/j.ydbio.2005.06.001
891 Sefc, K. M., Brown, A. C., & Clotfelter, E. D. (2014). Carotenoid-based coloration in cichlid
892 fishes. *Comp Biochem Physiol A Mol Integr Physiol, 173C*(100), 42-51.
893 doi:10.1016/j.cbpa.2014.03.006
894 Ser, J. R., Roberts, R. B., & Kocher, T. D. (2010). Multiple interacting loci control sex
895 determination in lake Malawi cichlid fish. *Evolution, 64*(2), 486-501.
896 doi:10.1111/j.1558-5646.2009.00871.x
897 Steiner, C. C., Rompler, H., Boettger, L. M., Schoneberg, T., & Hoekstra, H. E. (2009).
898 The genetic basis of phenotypic convergence in beach mice: similar pigment
899 patterns but different genes. *Mol Biol Evol, 26*(1), 35-45.
900 doi:10.1093/molbev/msn218
901 Subramanian, A., Tamayo, P., Mootha, V. K., Mukherjee, S., Ebert, B. L., Gillette, M. A.,
902 . . . Mesirov, J. P. (2005). Gene set enrichment analysis: a knowledge-based
903 approach for interpreting genome-wide expression profiles. *Proc Natl Acad Sci U*
904 *S A, 102*(43), 15545-15550. doi:10.1073/pnas.0506580102
905 Svardal, H., Quah, F. X., Malinsky, M., Ngatunga, B. P., Miska, E. A., Salzburger, W., . .
906 . Durbin, R. (2020). Ancestral Hybridization Facilitated Species Diversification in
907 the Lake Malawi Cichlid Fish Adaptive Radiation. *Mol Biol Evol, 37*(4), 1100-1113.
908 doi:10.1093/molbev/msz294
909 Wagner, C. E., Harmon, L. J., & Seehausen, O. (2012). Ecological opportunity and sexual
910 selection together predict adaptive radiation. *Nature, 487*(7407), 366-369.
911 doi:10.1038/nature11144
912 Wainwright, P. C., Alfaro, M. E., Bolnick, D. I., & Hulsey, C. D. (2005). Many-to-One
913 Mapping of Form to Function: A General Principle in Organismal Design? *Integr*
914 *Comp Biol, 45*(2), 256-262. doi:10.1093/icb/45.2.256
915 Wang, C., Xu, J., Kocher, T. D., Li, M., & Wang, D. (2022). CRISPR Knockouts of pmela
916 and pmelb Engineered a Golden Tilapia by Regulating Relative Pigment Cell
917 Abundance. *J Hered, 113*(4), 398-413. doi:10.1093/jhered/esac018
918 Watt, B., van Niel, G., Raposo, G., & Marks, M. S. (2013). PMEL: a pigment cell-specific
919 model for functional amyloid formation. *Pigment Cell Melanoma Res, 26*(3), 300-
920 315. doi:10.1111/pcmr.12067
921 Williams, T. M., & Carroll, S. B. (2009). Genetic and molecular insights into the
922 development and evolution of sexual dimorphism. *Nat Rev Genet, 10*(11), 797-
923 804. doi:10.1038/nrg2687
924 Wright, S. (1917). Color inheritance in mammals - I. *J Hered, 8*, 224-235.
925 Xie, H., Zhou, F., Liu, L., Zhu, G., Li, Q., Li, C., & Gao, T. (2016). Vitiligo: How do oxidative
926 stress-induced autoantigens trigger autoimmunity? *J Derm Sci, 81*(1), 3-9.
927

928 **DATA ACCESSIBILITY:** Raw sequence data are available at

929 https://www.ncbi.nlm.nih.gov/bioproject/PRJNA955776. Additional data are available at

Dryad [link to be provided prior to publication]. Dryad files include phenotypic measures and genotypes used for quantitative trait loci mapping.

AUTHOR CONTRIBUTIONS

KEP and RBR designed the research. ACB, ECM, PJC, and NBR performed animal husbandry, photography, and collections. NBR prepared sequencing libraries. AAB, CM, ECM, ACB, RBR, and KEP analyzed data. AAB and KEP wrote the paper with edits from all authors.

939 **FIGURES WITH LEGENDS**

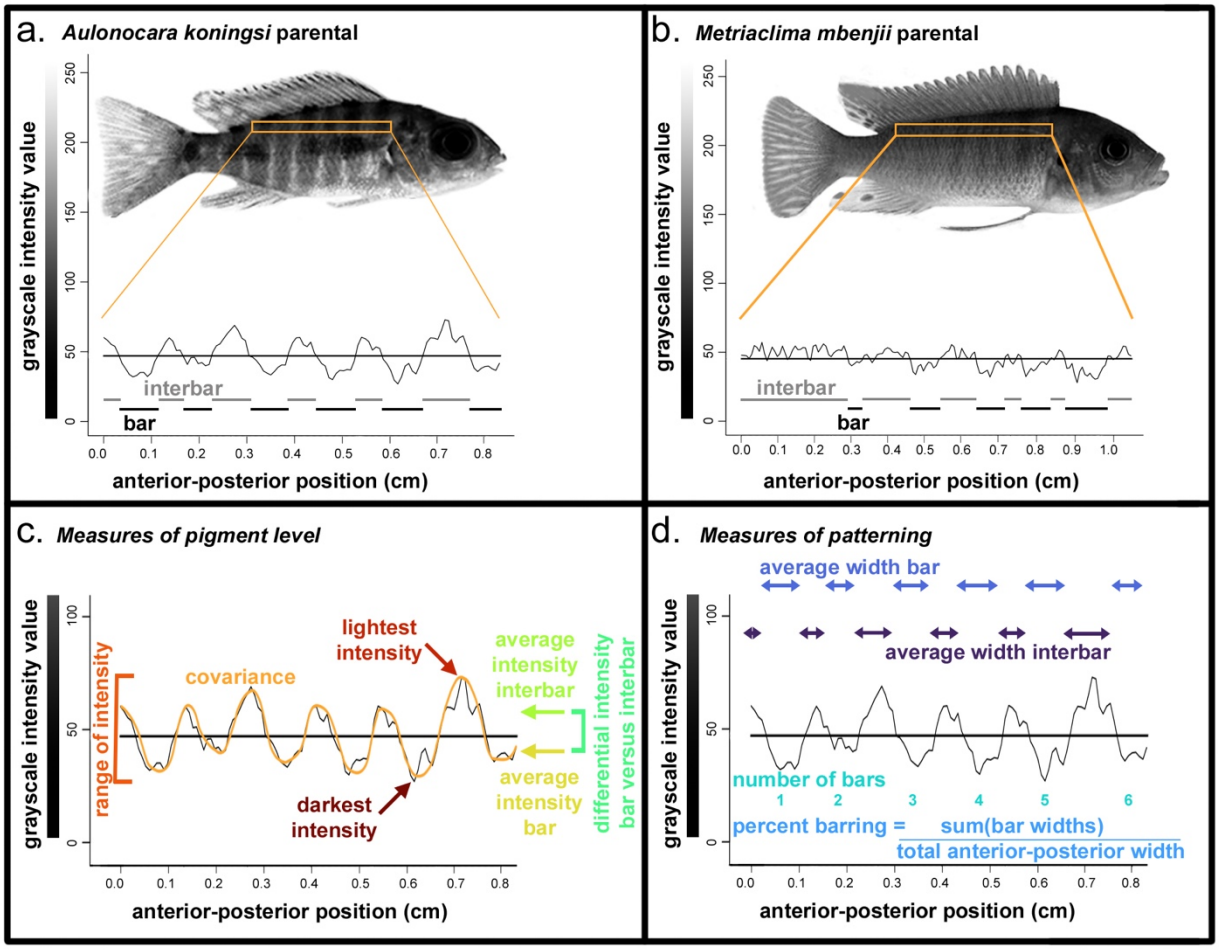

940

941 **Figure 1. Parental species and measures of variation in barring pattern and pigment**
942 **level.** Representative (a) *Aulonocara koningsi* and (b) *Metriaclima mbenjii* parental,
943 including quantification of region in orange rectangle into grayscale values. The horizontal
944 bar in graphs in (a) and (b) are the average grayscale intensity value, which was
945 calculated for each individual and used to characterize bar and interbars, indicated by
946 black and gray marks, respectively, in (a) and (b). From grayscale plots for each
947 individual, measures of (c) eumelanin pigment level and (d) bar patterning were
948 calculated as visualized. Colors in (c) and (d) match colors used in Figure 3.

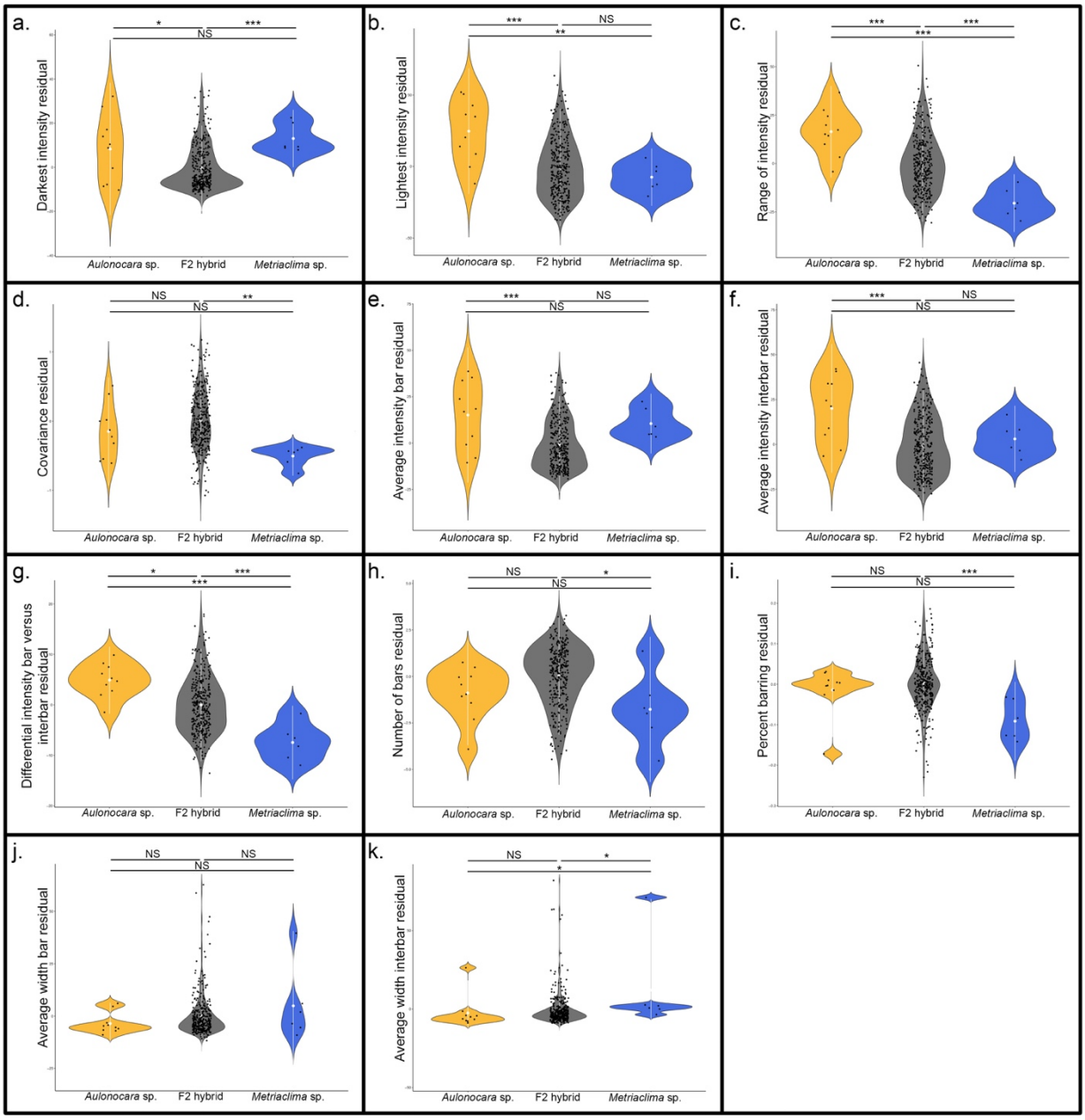

Figure 2. Variation in barring levels and patterns among *Aulonocara koningsi*, *Metriaclima mbenjii*, and their F_2 hybrids. One set of measures relates to pigment levels produced by melanophores and are (a) darkest intensity, (b) lightest intensity, (c) range of intensity, (d) covariance, (e) average intensity of bars, (f) average intensity of interbars, and (g) differential intensity bars versus interbars. A second set of measures

relates to the pattern of the bars and are (h) the number of bars, (i) percent barring, calculated as sum of total width of bars divided by total width of the isolated region, (j) average width of bars, and (k) average width of interbars. Significance in violin plots is based on ANOVA analysis followed by Tukeys HSD (data in Table S2; p-values indicated by * <0.05, ** <0.01, *** <0.005).

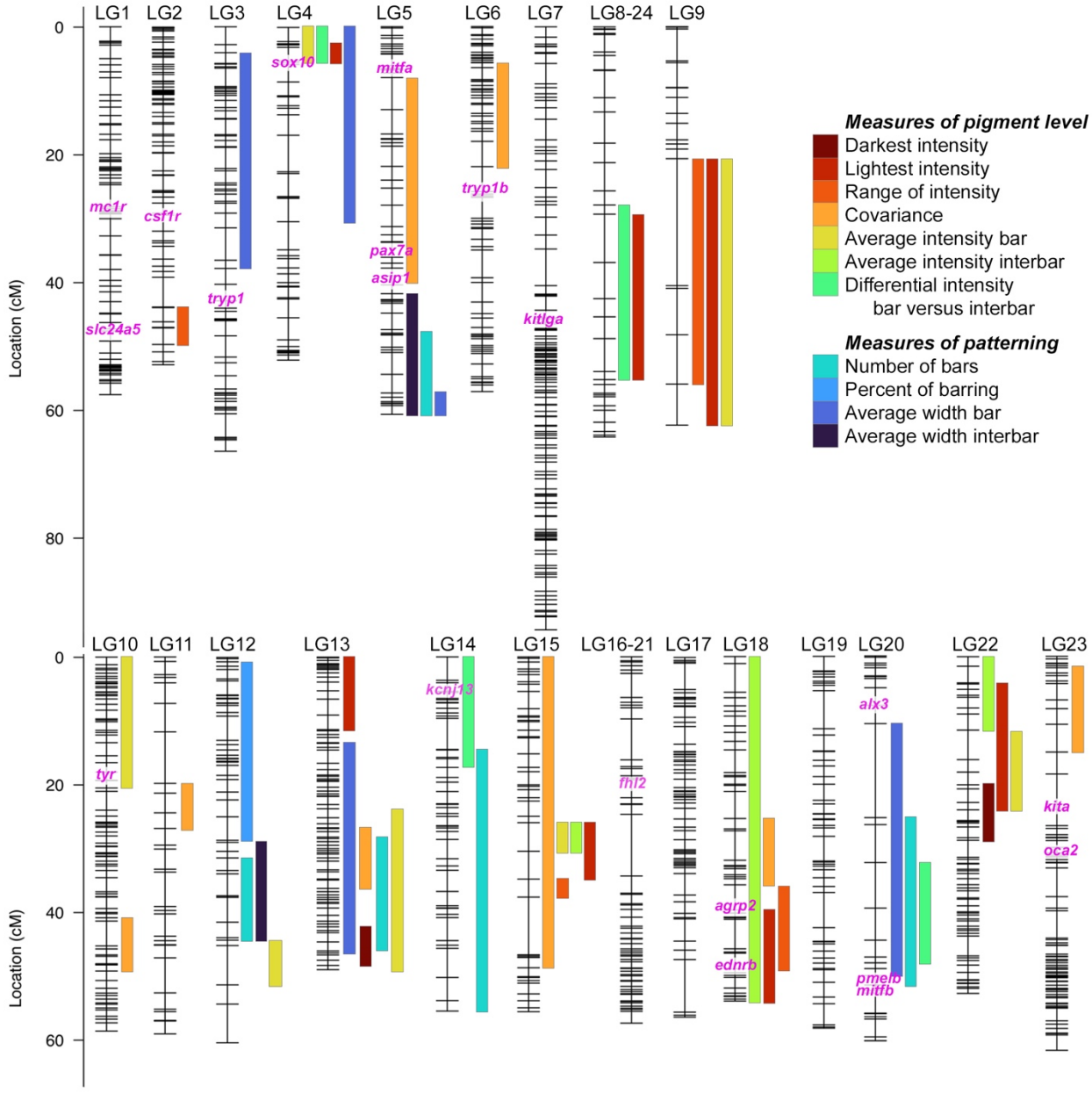

Figure 3. Quantitative trait loci (QTL) mapping identifies 48 intervals associated with variation in barring between *Metriaclima mbenjii* and *Aulonocara koningsi*. Each linkage group (LG, i.e., chromosome) has markers indicated by hash marks. Bar widths indicate 95% confidence interval for each QTL and bar color indicates the pigment trait analyzed. Candidate genes previously associated with variation in eumelanin

966 production and development of stripes or bars (see main text for references) are in pink
967 text, with their genomic locations indicated on linkage groups. Additional candidate genes
968 *pax3a* and *pmela* are located in unplaced scaffolds in the *M. zebra* UMD2a reference
969 genome and not included here. Illustrations of each trait are in Figure 1. QTL scans at the
970 genome and linkage group level are in Figures S2 and S3, respectively. Details of the
971 QTL scan, including statistical model and physical locations defining each QTL are in
972 Table S1.

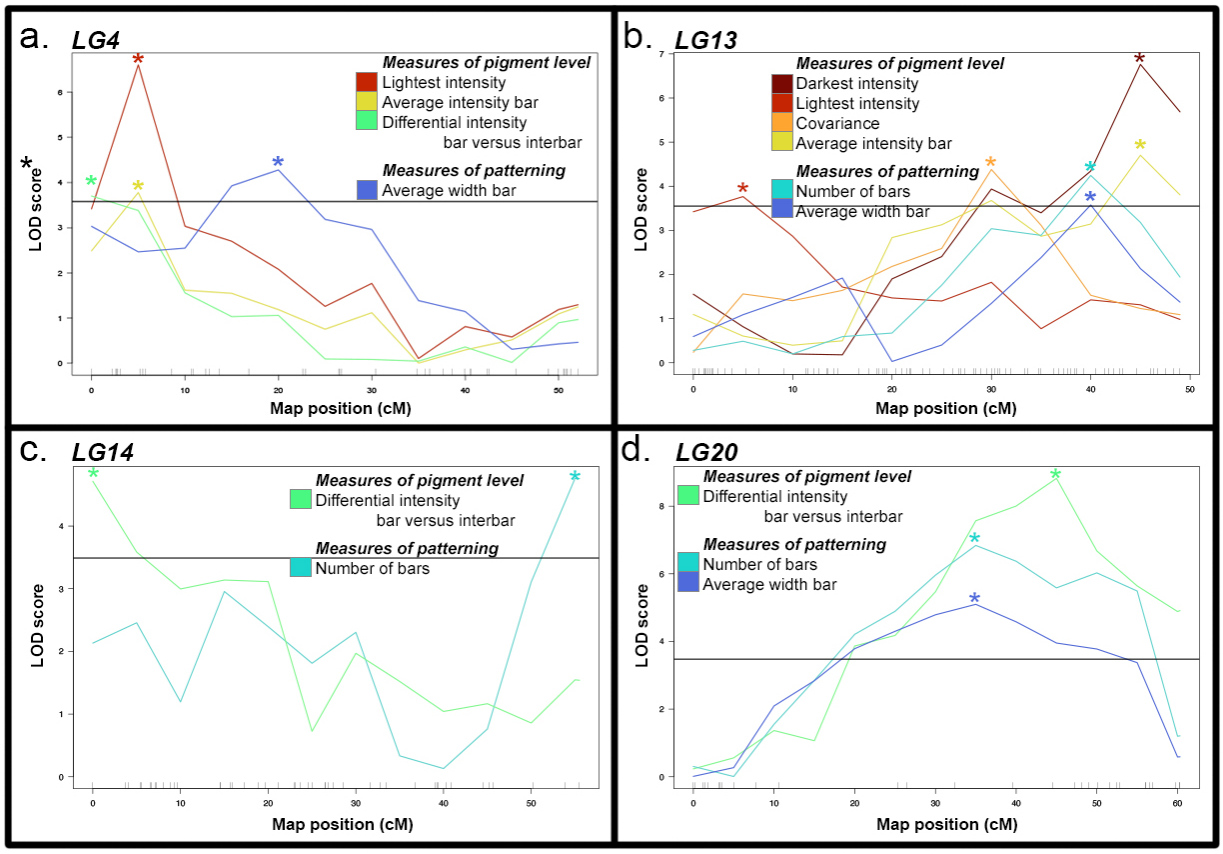

Figure 4. Quantitative trait loci (QTL) that underlie variation in pigment levels and pigment patterning are largely distinct. Included are all linkage groups—(a) LG4, (b) LG13, (c) LG14, and (d) LG20—in which QTL for pigment level and patterning have overlapping 95% confidence intervals as visualized in Figure 3. Colors represent trait, as indicated by the legend and as illustrated in Figure 1. Peak markers for each QTL are indicated by an asterisk in a color matching the trait. The solid horizontal line in each panel represents 5% significance, measured as the average value from each of the featured scans on that specific linkage group; averaging this significance did not cause any of these QTL to change from significant to non-significant or vice versa. Further details of the QTL are in Figure S3 and Table S1.